Video Article

Core/shell Printing Scaffolds For Tissue Engineering Of Tubular Structures

Marko Milojević[1], Boštjan Vihar[1,2], Luka Banović[2], Mihael Miško[2], Lidija Gradišnik[1], Tanja Zidarič[1], Uroš Maver[1,3]

[1]Institute of Biomedical Sciences, Faculty of Medicine, University of Maribor

[2]Institute for Development of Advanced Applied Systems (IRNAS)

[3]Department of Pharmacology, Faculty of Medicine, University of Maribor

Correspondence to: Marko Milojević at marko.milojevic1@um.si, Boštjan Vihar at bostjan.vihar@um.si

URL: https://www.jove.com/video/59951
DOI: doi:10.3791/59951

Keywords: Bioengineering, Issue 151, core/shell, coaxial, bioprinting, bioengineering, tissue engineering, CMC, alginate, tubular, tissue, engineering, vascularization

Date Published: 9/27/2019

Citation: Milojević, M., Vihar, B., Banović, L., Miško, M., Gradišnik, L., Zidarič, T., Maver, U. Core/shell Printing Scaffolds For Tissue Engineering Of Tubular Structures. *J. Vis. Exp.* (151), e59951, doi:10.3791/59951 (2019).

Abstract

Three-dimensional (3D) printing of core/shell filaments allows direct fabrication of channel structures with a stable shell that is cross-linked at the interface with a liquid core. The latter is removed post-printing, leaving behind a hollow tube. Integrating an additive manufacturing technique (like the one described here with tailor-made [bio]inks, which structurally and biochemically mimic the native extracellular matrix [ECM]) is an important step towards advanced tissue engineering. However, precise fabrication of well-defined structures requires tailored fabrication strategies optimized for the material in use. Therefore, it is sensible to begin with a set-up that is customizable, simple-to-use, and compatible with a broad spectrum of materials and applications. This work presents an easy-to-manufacture core/shell nozzle with luer-compatibility to explore core/shell printing of woodpile structures, tested with a well-defined, alginate-based scaffold material formulation.

Video Link

The video component of this article can be found at https://www.jove.com/video/59951/

Introduction

Arguably, the ultimate objective of tissue engineering (TE) is to produce functional tissues or organs in vitro, which can be used to regenerate or replace injured or diseased parts of the human body[1,2,3]. Current research in tissue engineering (TE) is focused on individual aspects of the field (scaffolding materials, fabrication procedures, cell sources, etc.)[4,5], as well as developing simple in vitro models of tissues and organs that mimic fundamental aspects of their in vivo counterparts. Such models are already useful for many applications, such as drug screening and toxicity studies, especially in cases where conventional 2D cell cultures fail to mimic the dynamic responses of the native tissues[6,7,8,9]. Three-dimensional in vitro models are usually constructed by combining cells[10], physico-chemical cues[11], and biologically active molecules[12,13] on scaffolds, which are obtained from decellularized tissues or constructed *de novo* from biological or biocompatible materials[14,15,16,17,18].

It is crucial that scaffolds recapitulate the complex 3D microarchitecture and hierarchical structure of the native tissues to enable functionality of the engineered tissues, representative of in vivo tissues[19]. Despite the significant technological advancement in TE, development of physiologically relevant artificial tissue constructs remains a challenge. Thick tissues (>200 µm in thickness) are especially problematic, due to limitations such as oxygen and nutrient diffusion[20]. Progress towards larger tissue constructs has been made; however, the required high proximity of cells to blood vessels in order to transport oxygen and nutrients and promote waste removal must be recapitulated. Vascularization of tissues (or alternatively, fabrication of interconnected 3D vascular networks within tissue constructs) plays a critical role in maintaining cell viability and promoting functions of in vitro engineered tissues, which is more difficult for models in prolonged experiments[21,22]. Furthermore, the required resolution, structural integrity, and simultaneous biocompatibility has yet to be achieved[23].

Several TE approaches have been proposed in an attempt to construct blood vessel-like structures and facilitate vascularization in vitro. Some examples include seeding endothelial cells (also co-cultured with other cells types such as fibroblasts) that self-assemble to generate microvascular networks[24], use of vascular progenitor cells and pericytes that promote endothelial cell growth[21,25], the delivery of angiogenic growth factors that induce vascularization[20,26], using cell sheet technology that allows for control over vascular layering[20], and fabrication of highly porous scaffold structures that promote angiogenesis[27]. The mentioned approaches focus on angiogenesis induction, which generally requires considerable amounts of additional growth factors (e.g., VEGF) and time to form. However, the biggest drawbacks are their limited reproducibility and restricted spatial control over vascular patterning, usually resulting in a random vasculature distribution within the tissue construct that does not necessarily facilitate perfusion.

Additive manufacturing (AM, such as 3D bioprinting) is increasingly involved in the fabrication of 3D constructs using biological or biocompatible materials to create scaffolds suitable for TE. Several AM approaches are being used and developed in parallel (e.g., ink jet- and microextrusion-based methods, different types of lithographic techniques) to produce scaffolds that mimic native tissues in their architecture, biochemistry, and functionality. The individual techniques exhibit certain advantages and disadvantages[28], which is why various modifications being explored

(e.g., micro-patterning, induced angiogenesis, etc.) to increase the extent to which large, complex, and stable vascular networks can be fabricated[22,29,30].

Among these, extrusion bioprinting is the most commonly used method, especially due to the broad range of compatible materials (a generally cell-friendly process[28,31,32]) as well as exceptional versatility in terms of applications (e.g., embedded and sacrificial printing[23,33], fabrication of hollow structures[34,35], etc.). The main challenges preoccupying present studies include the transfer from 2D to 3D structures, formation of a dense network of hollow tubes with high spatial resolution, and overall mechanical integrity and shape fidelity during fluid flow in cell culture conditions[30].

The most straightforward approach to perfusable tissue is the fabrication of an interconnected network of channels within the construct. The creation of such perfusable channels within a tissue scaffold is expected to solve many of the aforementioned problems, as it immediately allows for nutrient and oxygen diffusion while removing waste products. Therefore, the potential formation of necrotic regions within the construct is avoided[36]. Such channels may additionally be seeded with endothelial cells (ECs) and serve as artificial blood vessels in 3D tissue models[37]. In the most elementary sense, a vessel can consist of a hollow channel, soft layer of ECs, and stiff shell. Recently, 3D extrusion of two different materials in a core/shell fashion utilizing co-axial needles for extrusion has gained much interest[38,39,40,41], as it allows for fabrication of hollow tubes.

Similar to conventional microextrusion 3D printing, core/shell printing is performed with a co-axial nozzle (e.g., two needles with different diameters aligned on the same axis in a manner, so that the wider needle encloses the narrower one). Thus, two materials can be extruded simultaneously, with one as the central filament or “inner” core and a second as the “outer” shell[41]. To date, co-axial bioprinting has been utilized to fabricate structures with solid[42], core/shell[43], and hollow strands[40,44]; however, the materials used have not been optimized for both optimal cell viability and mechanical robustness of the printed constructs. As mentioned, the technique provides the possibility to combine biomaterials with different mechanical properties, in which the stiffer one supports the softer one. More importantly, if the scaffold material (e.g., alginate, carboxymethyl cellulose) is extruded as the shell, while the core composed of the cross-linking agent (e.g., calcium chloride) is dispensed from the inner capillary then rinsed out post-printing, it is possible to fabricate a continuous hollow tube in a single step[45].

With this in mind, a simple and repeatable one-step method was developed to build well-defined and perfusable scaffolds for the engineering of vascular structures and other tubular tissues. To develop a cost-effective technology, fabrication should ideally be a single-step process. Therefore, a core/shell set-up was adapted and integrated into the 3D bioprinter. The basic design consists of a central nozzle made of metal to avoid deformation during injection, around which a second nozzle of a larger diameter is placed. Such a co-axial nozzle set-up allows for co-extrusion of the two flows and immediate cross-linking of the extruded hydrogel channel. This enables direct fabrication of multilayered hollow filaments, while subsequent cross-linking with higher concentrations of calcium chloride ($CaCl_2$) ensure more permanent stabilization from the outside.

As such, this method allows for concurrent printing of scaffolds and microchannels, in which the hollow hydrogel filaments serve as a scaffold to support the mechanical integrity of 3D constructs and simultaneously act as built-in microchannels to deliver nutrients for cell growth. This protocol provides a detailed procedure of the core/shell 3D bioprinting strategy based on use of a custom-made co-axial nozzle in which hydrogel 3D structures with built-in channels are fabricated by controlling cross-linking to produce hollow filaments, which remain perfusable during cell culture.

The 3D printing set-up used in this work is configured as previously described by Banović and Vihar[46] and can be divided into three main components: A) a three-axis CNC mechanical set-up with 50 µm positioning accuracy in the X, Y, and Z directions; B) two extruders, adapted for disposable, 5 mL luer-lock syringes, with 1.2 µL voxel resolution; and C) controlling electronics and software.

To facilitate core/shell printing, an appropriate nozzle was developed that can be mounted on one of the extruders (primary extruder, printing the core) and is compatible with G27 blunt-end needles. It also has luer-lock compatibility to connect with the second extruder (printing the shell). The first prototypes were fabricated by inserting a blunt-end G27 needle (inner diameter = 210 µm, outer diameter = 410 µm) into either a G21 needle (inner diameter = 510 µm, outer diameter = 820 µm) or G20 conical tip (inner diameter = 600 µm), then inserting a secondary needle laterally to supply the shell material. However, due to slight bending of the needle shaft, it is not possible to produce a nozzle tip with concentric alignment of the inner and outer needles.

To solve this issue, a new nozzle design was devised that fulfilled the following criteria: 1) it can be manufactured using a 3-axis CNC mill, 2) it can be made from various materials (high performance plastics, such as PEEK or metals), 3) it has luer-lock compatibility for applying shell material, and 4) is compatible for a G27 blunt-end needle and holds it in place at two positions to align the tip with the central axis. A schematic of the nozzle prototype is shown in **Figure 1**.

Protocol

1. Preparation of hydrogels and cross-linking solutions

1. Briefly, by vigorously mixing, dissolve ALG and CMC powders in ultra-pure water to obtain a total 3 wt% ALG and 3 wt% CMC solution.
   NOTE: In this work, 5 mL syringes are used for printing; thus, the final amount of material is adjusted to that volume. However, for other extrusion cartridges and printed sample sizes, the amount of prepared material should be scaled accordingly.
2. Add 1.5 wt% cellulose nanofibers to the ALG-CMC mixture for additional mechanical reinforcement to reach the desired viscosity, suitable for printing.
3. Agitate the hydrogel suspension until homogeneous using an overhead mixer.
   NOTE: No fibers or bubbles should be present in the hydrogel.
4. Prepare 10 mL of 100 mM calcium chloride ($CaCl_2$) solution in ultra-pure water, which is used as the primary cross-linking solution for printing.

5. Prepare 10 mL of 5 wt.% $CaCl_2$ solution in ultra-pure water, which is used as a secondary cross-linking solution in post processing of scaffolds.
   NOTE: Generally, all hydrogel formulations, which are suitable for immediate chemical cross-linking, allow for one-step fabrication of hollow tubes and can be used with this type of core/shell set-up. The printing and cross-linking mechanisms need to be optimized accordingly. Viscosity of the hydrogel will vary depending on the desired composition; however, it can be adjusted with polymer concentrations and the addition of thickening agents (e.g., nanofibers). The ideal viscosity for 3D printing of stable structures is high enough for the extruded filament to retain its shape and for the scaffold to hold its own weight before cross-linking.

2. Core/shell printing of perfusable scaffolds

1. Prior to printing, sterilize the bioprinter by spraying 70% ethanol thoroughly and expose it to UV light for 1 h.
2. Turn on the bioprinter and run the controlling software, which comes in a bundle with the 3D printer.
3. Perform the homing procedure by pressing the **Home** icon.
4. Using the toolbar command **File | Import G-Code**, import the generated scaffold g-code.
5. Transfer the hydrogel to a sterile 5 mL syringe and place it in one of the extruder mounts of the 3D printer. Via the luer-lock and a short tube, connect it to side luer input of the core/shell nozzle.
6. Transfer the cross-linking solution (100 mM $CaCl_2$) to another sterile 5 mL syringe with an attached G27 blunt-end needle and insert it into the top needle holder of the core/shell nozzle. The inner needle should slightly protrude (~1 mm) from the outer core/shell nozzle. Adjust the alignment manually. Insert the second syringe in the extrusion mount.
7. To correctly insert the syringes into the mounts (set-up shown in **Figure 2**), manually control both extrusion mounts by clicking the **A and B** and **Up and Down** arrows.
8. Before the printing starts, separately extrude the hydrogel and the cross-linking solution to clear all excess air bubbles in the core/shell nozzle and ensure a continuous hydrogel flow.
9. Using the **Z** and **Up and Down** arrows, manually adjust the distance between the nozzle and printing substrate. It is recommended to use a flat, glass-printing substrate, which has good adhesion. The extrusion nozzle should not be in contact with the substrate to allow for uninterrupted flow of the hydrogel. The optimal distance between the nozzle and substrate (layer height) is typically the same as the width of the outer nozzle diameter, but it is adjusted to the material used and individual printing parameters. Adjust the starting printing height according to individual needs.
10. Press the **Play** button to start the printing process.
    NOTE: It is recommended to include the printing of a skirt (**Figure 3**) surrounding the scaffold to ensure the laying of a homogenous hollow filament before printing of the actual scaffold starts. To achieve optimal hydrogel flow with the intention to print optimal scaffolds, vary formulation composition, cross-linking solution composition, and printing parameters (i.e., printing speed, extrusion pressure, printing temperature, distance between the substrate and extrusion nozzle, etc.).
11. After printing, carefully remove the substrate with the printed scaffold and pour the secondary cross-linking solution (5 wt.% $CaCl_2$) over the entire scaffold to ensure the cross-linkage over the entire scaffold. Incubate for 1 min at room temperature (RT).
    NOTE: Make sure that the entire scaffold is submerged in the cross-linking solution. This step is crucial for achieving desired strength properties of the scaffold but will vary depending on the material and cross-linking method used.
12. Using a scalpel manually cut the excess skirt material.
13. Sterilize the scaffolds under an UV light for 30 min. Carefully flip the scaffold and repeat the sterilization process.
14. Carefully detach the scaffold from the substrate by gently pulling it sideways. If the scaffold adheres strongly to the substrate, separate it by inserting a sharp edge between them.
15. Transfer the scaffold into a colorless cell culture media (DMEM supplemented with 5 wt.% FBS, 100 U/mL penicillin and 1 mg/mL streptomycin), and incubate them at 37 °C in an atmosphere containing 5 wt.% CO_2 for at least 24 h.

3. Preparation of endothelial cells and live/dead assay solution

1. For cell culturing, prepare the advanced DMEM cell culture medium with added phenol red and supplement it with 5 wt.% FBS and 2 mM L-glutamine. Add 100 U/mL penicillin and 1 mg/mL streptomycin.
2. Initiate the human umbilical vein endothelial cell (HUVEC) line and passage them in accordance with HUVEC culturing protocols as described[47].
   NOTE: It is recommended to culture the cells in cell culture media with added phenol red for simple visualization during injection of the cells into white translucent scaffolds as described below.
3. For cell counting, pipette 100 µL of cells suspended in cell culture media and stain them with 900 µL of 0.1 wt.% trypan blue solution.
4. Use an automated cell counter or manual hemocytometer to count and obtain the estimated number of cells in suspension.
5. For the live/dead assay, prepare a solution of 4 mM Calcein-AM and 2 mM propidium iodide in sterile PBS.
   NOTE: The live/dead solution should be prepared directly before conducting the assay.

4. Transferring cells into scaffolds

1. Remove the scaffolds from cell culture media and transfer them into a sufficiently large glass Petri dish.
2. Immediately before injecting the cells into the scaffolds, dissociate the HUVECs from the flasks using treatment by 0.25 wt.% trypsin.
   1. Briefly, dispose cell culture media and incubate the cells with 0.25 wt.% trypsin (~2 mL) for 5 min at 37 °C.
   2. After incubation add ~3 mL of cell culture media to the trypsinized cells and transfer all detached cells to a centrifuge tube.
   3. Centrifuge the cells at 200 x *g* for 5 min and dispose of the supernatant.
   4. Resuspend the cells in fresh cell culture media.

3. Count the cells as described previously. Adjust the total cell concentration according to individual needs. In this work, a starting concentration of 340,000 cells/mL is used.

4. Resuspend the cells in a sterile syringe with an attached blunt G27 needle.
5. Find an entry point and start carefully injecting cells into the scaffolds. The cell suspension flow through a translucent scaffold should be visible. Make sure that the entire scaffold fills up with cell suspension.
6. Submerge the scaffolds in cell culture media and incubate them at 37 °C in an atmosphere containing 5 wt.% CO_2 for up to 10 days.
7. Replenish the cell culture media according to experimental needs.

5. Live/dead assay and cell imaging

1. After incubation, rinse the scaffolds with PBS.
2. With a blunt-end needle, carefully inject the previously prepared live/dead solution (4 mM calcein-AM and 2 mM propidium iodide in PBS) into the scaffolds and incubate them in PBS for 30 min at 37 °C. Make sure that the solution flows through the length of the entire scaffold.
3. Rinse the scaffolds with PBS.
4. Carefully transfer the scaffolds to a glass slide.
5. Observe the dyed cells directly in the scaffolds under a fluorescence microscope.
   NOTE: Viable cells produce green fluorescence and dead cells emit red fluorescence light.

Representative Results

The aim of this work was to develop an easy-to-manufacture core/shell nozzle with luer-compatibility for core/shell printing of woodpile structures. In addition, a straightforward and repeatable one-step printing protocol was described, which is simple to modify and accommodates a broad range of materials and different chemical cross-linking mechanisms to build well-defined and perfusable scaffolds for engineering of vascular and other tubular tissue structures.

Core/shell nozzle
The nozzle is composed of a G27 blunt-end needle (for printing the inner axial filament) and the nozzle body, which holds the needle in place and creates an outer nozzle for the shell filament with a connection port for material input. A schematic is shown in **Figure 1**. Two 5 mL syringes, which are placed into the individual extruders and provide the core and shell materials. Tubing connects the nozzle body with the syringe, providing the shell material.

The complete assembly of the core/shell nozzle and syringe set-up is shown in **Figure 2**. The first functional prototype of the nozzle body was manufactured by CNC milling a block of polyoxymethylene (POM). Compatibility and sealing between the element, a G27 needle and tubing was tested by installing into Vitaprint. No leakage of the shell material was observed in the nozzle, luer-lock connector, or between body and needle. The nozzle body fits tightly with the needle hub (luer connector), ensuring synchronized motion of the whole nozzle with the extruder.

Scaffold building
The most straightforward approach to fabricating scaffolds is by depositing materials layer by layer where printing direction is changed every consecutive layer, typically at an angle of 90°. Due to the visco-elastic and hygroscopic properties of the hydrogels, retaining shape fidelity of the printed structures remains challenging. The main purpose of this protocol section is 3D printing of perfusable core/shell scaffolds using two polymers, which have previously shown promising results for scaffold building (ALG and CMC) with the addition of cellulose nanofibers (NFC) for increased mechanical stability. Both ALG and CMC are negatively charged, water-soluble linear copolymers[48] and both contain carboxyl groups, which can be cross-linked with the addition of divalent cations. Ca^{2+} particles form ionic bonds with two functional groups simultaneously, forming connections between polymer chains, increasing gel rigidity.

Printing of perfusable scaffolds
The aim of this process is to 3D-print simple woodpile scaffold structures, which span over several layers and retain their shape fidelity as well as perfusability until becoming fully cross-linked. This requires even coextrusion of core and shell without crossover or retraction movements, which can interrupt the flow. Therefore, typical CAD modelling and slicing methods are less suitable. In this work, a manually designed g-code is used, and a python-based g-code generator was developed for fast g-code preparation.

The scaffolds were structured in a woodpile grid shape and built on a flat glass surface. The fabrication was performed layer-by-layer, depositing the crossing lines of each succeeding layer in an angle 90° to the previous one. Additionally, each succeeding layer was 2% narrower in the X and Y directions, ensuring continuous filament support by preceding layers. The distance between filaments (macropore size) can be precisely designed in the g-code by taking into account the outer diameter of the extruded filament (0.8 mm) and the distance between gridlines (3 mm).

Scaffolds were required to fulfill key inclusion criteria for further consideration. First, scaffolds with at least 4 layers in height were required to retain their structural integrity and geometry (e.g., macropore size) during printing, to be eligible for further development. Second, scaffolds needed to remain perfusable (stable microchannels) even after being incubated for 7 days in cell culture media at 37 °C. At appropriate time intervals (1, 2, 5, and 7 days) scaffolds were taken out of the culture media and tested to see if they were still perfusable. In **Figure 4A**, the cross-section of a freshly printed and post-processed scaffold displays a clearly visible hollow channel inside the filament. In **Figure 4B**, it is clear that even after 72 h incubation in cell culture media at 37 °C, the filament retains the hollow structure through the entire scaffold length.

Several formulations were printable, remained structurally stable, preserved the printed geometry, and remained perfusable; however, a single one was chosen for further testing (i.e., 3 wt.% ALG + 3 wt.% CMC + 1.5 wt.% NFC), which allowed printing of perfusable scaffolds with up to 10 layers. The printing process with the custom nozzle is shown in **Figure 5A**. Core/shell printing was possible with less viscous formulations; however, gels with higher concentrations did not allow continuous flow through the nozzle. For primary cross-linking (core material, delivered during printing) 100 mM $CaCl_2$ was utilized, which adequately stabilized the continuous formation of a hollow filament, without causing gel solidification within the nozzle. Post-printing, the scaffolds were soaked in a 5 wt.% $CaCl_2$ solution to completely cross-link the hydrogel for long-term shape fidelity. A finished scaffold sample is pictured in **Figure 5B**. During the optimization, process of the formulation an artificial dye was used in the core solution, to allow visual evaluation and examining the quality of the extruded filament. The dye was not used for the fabrication of the final scaffolds, which were prepared for cell seeding and cultivation.

Live/dead assay

After incubation, a live/dead assay was used to visualize the ECs and distinguish between the living (green) and the dead (red) cells within the incubated scaffold. This served two main purposes: A) to determine whether the scaffolds provide a biocompatible environment to promote growth and adhesion without exhibiting harmful effects on the cell, and B) to visualize the structural integrity of tubular structures and their internal channel system in more detail.

The results of the live/dead assay are shown in **Figure 6**. In the presence of intracellular esterases, the plasma membrane permeable Calcein-AM is converted to Calcein, emitting green fluorescence light in live cells. On the other hand, apoptotic cells are visualized by membrane impermeable propidium iodide, which fluoresces in red when intercalated in the DNA double helix. Live/dead images and bright-field pictures of scaffolds were combined to help visualize the cells inside the hollow channels. The staining solution was injected, and the assay performed directly in the 3D printed scaffolds after scaffold-cell incubation for 48 h.

It should be noted that a relatively small seeding density of ECs was used (340,000 cells/mL), as this study served only as a proof-of-concept for core/shell printing of perfusable scaffolds. The most significant conclusion of the live/dead assay is that even after 48 h, no dead cells (red) were observed, proving that neither the scaffold material itself, nor its degradation products exhibited toxic effects. Furthermore, the ECs did in fact adhere and remain attached inside the scaffolds and seemed to form evenly distributed agglomerates when grown inside the channels. This suggests that the described fabrication method and scaffold formulation provide a suitable framework for building in vivo, relevant, tubular tissue morphologies. Besides mimicking cell-ECM interactions and tight cell-cell communication in all three spatial dimensions, complex tissue engineering also requires constant cell exposure to fresh medium to sustain their viability. This in turn can be achieved by a dense channel network under continuous perfusion, which warrants further investigation in future work, and will require optimizing material and growth parameters to facilitate long-term tissue engineering of vasculature.

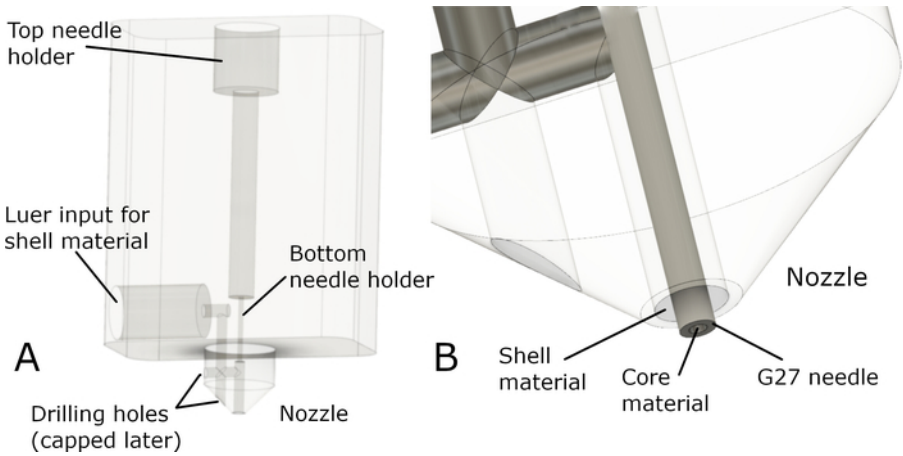

Figure 1: Core/shell nozzle prototype. (A) The overall design and the main components of the nozzle body prototype are shown. The nozzle is completed by inserting a blunt-end G27 needle through the top. The top and bottom needle holders immobilize and realign the needle with the nozzle axis, ensuring that the tip extends from the nozzle through the center. To connect the nozzle with "shell" material extruded from the secondary syringe, tubing with a luer-lock connector is attached to the lateral input. From here, the material is forwarded to the nozzle through a narrow channel. The fabrication of the mentioned channel requires drilling in two positions, producing holes that need to be capped after manufacturing). **(B)** Shown is a close-up of the nozzle with an inserted G27 needle, extending out of the nozzle. Please click here to view a larger version of this figure.

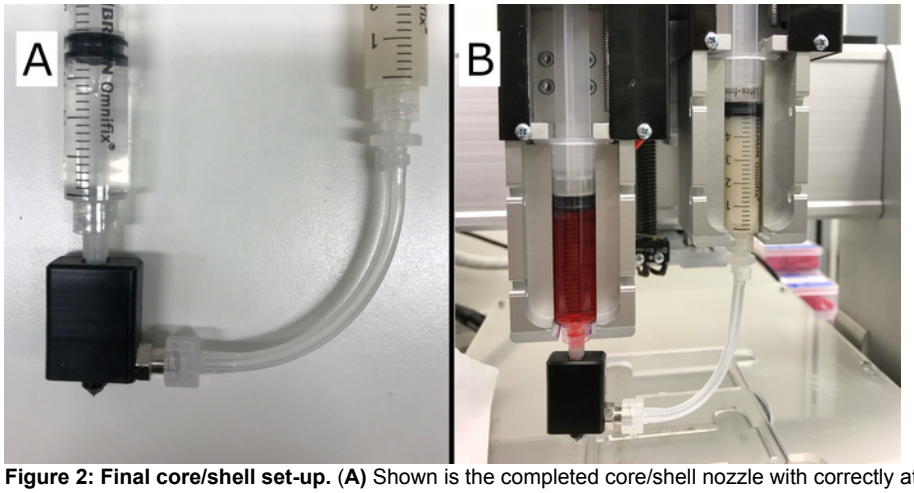

Figure 2: Final core/shell set-up. (**A)** Shown is the completed core/shell nozzle with correctly attached syringes containing the hydrogel (right), building the "shell" and cross-linking solution (left) extruded as the "core". (**B)** Shown is the core/shell set-up installed into the Vitaprint system with two extruders. Please click here to view a larger version of this figure.

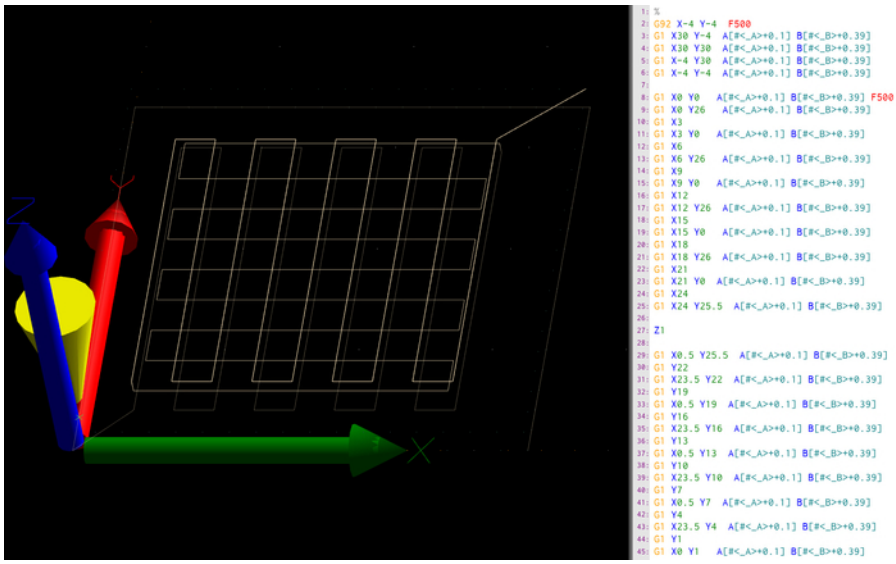

```
%
G92 X-4 Y-4 F500
G1 X30 Y-4 A[#<_A>+0.1] B[#<_B>+0.39]
G1 X30 Y30 A[#<_A>+0.1] B[#<_B>+0.39]
G1 X-4 Y30 A[#<_A>+0.1] B[#<_B>+0.39]
G1 X-4 Y-4 A[#<_A>+0.1] B[#<_B>+0.39]

G1 X0 Y0 A[#<_A>+0.1] B[#<_B>+0.39] F500
G1 X0 Y26 A[#<_A>+0.1] B[#<_B>+0.39]
G1 X3
G1 X3 Y0 A[#<_A>+0.1] B[#<_B>+0.39]
G1 X6
G1 X6 Y26 A[#<_A>+0.1] B[#<_B>+0.39]
G1 X9
G1 X9 Y0 A[#<_A>+0.1] B[#<_B>+0.39]
G1 X12
G1 X12 Y26 A[#<_A>+0.1] B[#<_B>+0.39]
G1 X15
G1 X15 Y0 A[#<_A>+0.1] B[#<_B>+0.39]
G1 X18
G1 X18 Y26 A[#<_A>+0.1] B[#<_B>+0.39]
G1 X21
G1 X21 Y0 A[#<_A>+0.1] B[#<_B>+0.39]
G1 X24
G1 X24 Y25.5 A[#<_A>+0.1] B[#<_B>+0.39]

Z1

G1 X0.5 Y25.5 A[#<_A>+0.1] B[#<_B>+0.39]
G1 Y22
G1 X23.5 Y22 A[#<_A>+0.1] B[#<_B>+0.39]
G1 Y19
G1 X0.5 Y19 A[#<_A>+0.1] B[#<_B>+0.39]
G1 Y16
G1 X23.5 Y16 A[#<_A>+0.1] B[#<_B>+0.39]
G1 Y13
G1 X0.5 Y13 A[#<_A>+0.1] B[#<_B>+0.39]
G1 Y10
G1 X23.5 Y10 A[#<_A>+0.1] B[#<_B>+0.39]
G1 Y7
G1 X0.5 Y7 A[#<_A>+0.1] B[#<_B>+0.39]
G1 Y4
G1 X23.5 Y4 A[#<_A>+0.1] B[#<_B>+0.39]
G1 Y1
G1 X0 Y1 A[#<_A>+0.1] B[#<_B>+0.39]
```

Figure 3: G-code of the tubular scaffold. Here a screenshot of the printer software is shown, specifically the path preview (**A**) and raw g-code of the first layer (**B**). The g-code is a set of instructions with target coordinates in absolute spatial directions (X, Y, Z), as well as extrusion (A,B) in relative directions. The G command determines the type of instruction, whereas G1 represents linear movement towards the target coordinates and G92 determines the initial starting position. In addition, the feed-rate of following commands is determined with instruction F in mm/min. Please click here to view a larger version of this figure.

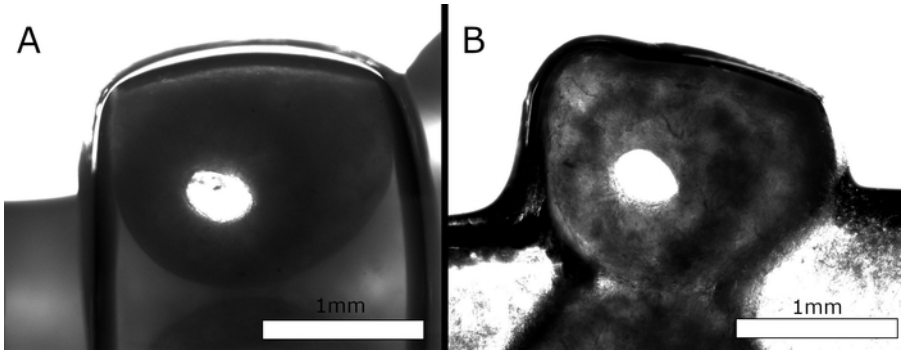

Figure 4: Cross-section of a scaffold strand with a hollow interior. (**A)** Shown is the cross-section slice of the freshly printed and post-processed scaffold. (**B)** Shown is the cross-sectional slice of the scaffold after being incubated in cell culture media for 72 h. While the nozzle shape defines the extrusion of a tube with a round cross-section, the filament appears to be somewhat flattened on deposition. The internal channel, however, stays intact and retains its form during incubation. Please click here to view a larger version of this figure.

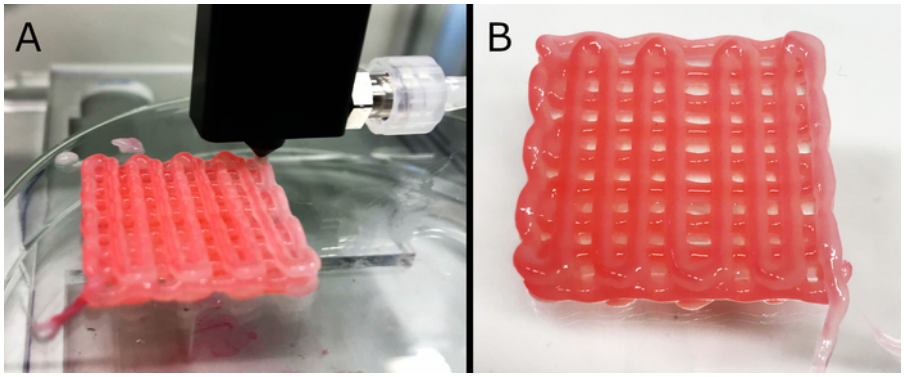

Figure 5: Core/shell printing of scaffolds. Here, fabrication (**A**) of a three-layered hollow-tube scaffold and its final form (**B**) are shown. For improved visualization, the cross-linking solution in the core was stained with a red dye. The formulation exhibits sufficient mechanical stability to retain scaffold stability, even if thicker structures (up to 10 layers, data not shown) are fabricated. The outer dimensions of the final structure were approximately 27 mm x 27 mm x 3.5 mm. Please click here to view a larger version of this figure.

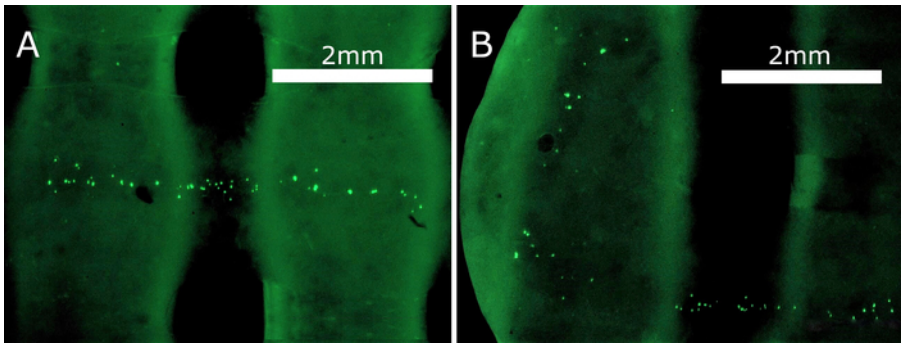

Figure 6: Live/dead assay performed directly in the scaffolds. A suspension of HUVECs was injected into the inner scaffold channel, incubated for 48 h, and treated with live/dead dye. Viable HUVECs emit green fluorescence light, which is represented in the bright spots of the image. Dead cells emit green fluorescence light; however, none are visible in the observed scaffold. The distribution of the cells also signifies the shape and retained perfusion capabilities of the channels. To a minor extent, the live/dead assay solution also stained the scaffolding material, producing light fluorescence under the microscope. Please click here to view a larger version of this figure.

Discussion

Nozzle design

Using the developed core/shell nozzle, integrated into a two-extruder Vitaprint system, hollow, tubular scaffolds were fabricated in a single-step process. To achieve an even thickness of the tube wall through most of the prepared scaffolds, the needle needs to be positioned centrally on the axis of the outer extrusion ring. Standard gauge needles often exhibit a slight, yet significant eccentricity off the axis. Thus, the nozzle body was designed to hold the needle in two places, once at the top (fixing the hub) and once before the final core/shell chamber (fixing the cannula itself), correcting its axial alignment. The precision of the axial alignment increases with the distance between the fixation point. There is, however, a tradeoff between needle length and available nozzle chamber volume. To improve functionality of the set-up further, certain modifications of the nozzle can be implemented: A) a nozzle mount with improved stability, B) additional nozzles for a wider range of needle compatibility, C) a precise adjustment mechanism for needle to nozzle positioning, and D) integrating additional inputs and microfluidic devices for on the fly material preparation.

Hydrogel optimization

To determine the optimal ALG:CMC ratio, several material iterations were evaluated. Generally, core/shell printing with concentrations above 3 wt.% of both components was rendered impossible, because it did not allow for a continuous hydrogel flow or resulted in clogging of the nozzle. Specifically, ALG concentration above 3 wt.% increased the viscosity excessively and resulted in nozzle clogging, while lower ALG concentrations and higher CMC (>3 wt.%) concentrations slowed down cross-linking times and thus failed to provide sufficient structural support of the scaffold. Core/shell printing was possible with less viscous formulations; however, extruded gel viscosity must be sufficient to sustain long term shape fidelity. In the end, a 1:1 ALG:CMC ratio was proven to be the most suitable choice which confirms a previous study by Maver et al.[49]. The addition of NFC significantly improved printability and structural rigidity of core/shell printed scaffolds but had no significant effect on cross-linking properties of the material.

Custom applications, optimized for specific cell types and experimental set-ups will require well-tailored scaffolding materials, which will vary in composition and cross-linking mechanisms. The method described in this work is based on an alginate-cellulose mixed polymer solution, which is cross-linked ionically using Ca^{2+} ions. Alginate itself is a linear polymer of blocks of (1,4)-linked β-d-mannuronate (M) and α-l-guluronate (G) residues that can be reversibly ionically crosslinked by application of Ca^{2+} and other divalent cations such as Sr^{2+}, Br^{2+}, Mg^{2+}. Nevertheless, the most widely used ion for cross-linking of alginate remains Ca^{2+} in the form of $CaCl_2$. Ca^{2+} can also be used in the form of $CaSO_4$ or $CaCO_3$;

however, the low solubility of $CaSO_4$ relative to $CaCl_2$ means slower gelation. $CaCO_3$ yields even slower gelation times which can result in weak and inconsistent mechanical properties.

Longer gelation times typically produce a more homogenous construct, however, certain applications, such as core/shell printing requires fast gelation rates[50]. Mg^{2+} ions also induce gelation; however, their cross-linking efficiency is about 5x-10x lower, compared to Ca^{2+}, with cross-linking times of 2-3 h. In addition, magnesium ions are more selective towards guluronic units, hence the cross-linking depends more on the chemical composition of the ALG[51]. In this case, a fast gelation rate is essential to ensure continuous hollow channel formation before the hollow structure can collapse. $CaCl_2$ yields the fastest gelation rate, which is crucial for the direct deposition of hollow filaments. 100 mM $CaCl_2$ was utilized, which adequately stabilized the continuous formation of a hollow filament without causing gel solidification within the nozzle.

Printing and post-processing of scaffolds
The following steps should be considered during this portion of the process, including 1) ensuring that all solutions and materials including the 3D bioprinter are properly sterilized before printing. 2) When preparing the hydrogel, homogeneity of the material is crucial for continuous printing. Introduction of impurities or air bubbles should be avoided, as they can clog the nozzle and/or disrupt the extrusion. 3) The syringes should be properly connected to the core/shell nozzle via the luer-lock mechanism and correctly inserted in the extruder mounts as seen in **Figure 2A,B**. 4) Before printing a complex structure, it is recommended to pre-extrude a small portion of the gel and cross-linking solution to clear the excess air bubbles in the core/shell nozzle and ensure a continuous hydrogel flow. This can be incorporated directly into the g-code to improve repeatability. 5) It is helpful to add a skirt surrounding the scaffold to ensure the laying of a homogenous hollow filament before the printing of the scaffold itself starts.

Additionally, 6) to improve adhesion between the printing filament and substrate, it is recommended to use a flat surface with good adhesion (i.e., a glass slide or Petri dish). 7) The extrusion nozzle should not be in direct contact with the substrate to allow for uninterrupted flow of the hydrogel. The initial distance will strongly impact the quality of the print, but thickness of the extruded filament is a good approximation of the initial setting. 8) The starting printing height in the g-code should be adjusted according to individual needs. After the printing parameters are optimized, the scaffold g-code should be imported into Planet CNC software and the printing process started as described in the protocol. 9) To control and optimize hydrogel flow with the intention to print optimal scaffolds, both formulation composition and printing parameters should be varied (i.e., printing speed, extrusion pressure, printing temperature, distance between the substrate and extrusion nozzle, layer height, scaffold size, etc.).

In general, higher flow rates are required to print formulations with higher viscosity. As mentioned, all hydrogel formulations, which are suitable for immediate chemical cross-linking, allow for one-step fabrication of hollow tubes and may be used with the described core/shell set-up. The printing and cross-linking mechanisms need to be optimized accordingly. After printing, all scaffolds were post-processed by secondary cross-linking with 5 wt.% $CaCl_2$ solution, which assured complete cross-linking of the ALG-CMC component and sterilized from both sides under a UV light for at least 30 min. It should be ensured to completely engulf the scaffold with the cross-linking solution and incubate for long enough to complete the cross-linking process. Post-processing will differ based on the material and cross-linking mechanism used, which should be considered beforehand. After post-processing, scaffolds should be removed carefully from the substrate, transferred to cell culture media, and incubated in a controlled atmosphere for at least 24 h before cell seeding. Using a colorless medium will improve visibility of the cell suspension during injection into the scaffolds.

Live/dead assay
The live/dead solution should be prepared directly before conducting the assay and kept in the dark before conducting the assay, as it contains fluorescence dyes that are prone to bleaching. After the desired incubation time, the cell culture media should be carefully discarded surrounding the scaffolds and rinsed with PBS. Ideally, the same entry point should be used for cell seeding followed by the live/dead assay being injected into the scaffolds.

Importance of results
Both ALG and CMC have been already used to promote angiogenesis in vitro. Based on its ECM-mimetic features, physical cross-linking, and biocompatibility, ALG has been commonly employed as a component for delivery and controlled release of angiogenic growth factors (e.g., bFGF, HGF, VEGF164, and Ang-1*respectively)[52,53,54]. Furthermore, in combination with gelatine, CMC has also been used for encapsulating vascular endothelial cells due its rapidly cross-linking capabilities under physiological conditions[55]. NFC were added to further increase the mechanical stability and shape fidelity of scaffolds. It should be emphasized that the objective was not to enhance the vascularization but to demonstrate the possibility of producing perfusable, hollow ALG-CMC scaffolds, printed in core/shell fashion, which also facilitates the attachment and proliferation of HUVECs. The choice of using an ALG-CMC mixture was based on findings of commonly used, easily accessible, and biocompatible base materials that could enable core/shell printing of hollow channels. Many other materials may be more viable options for enhancing angiogenesis; however, some are not suitable for core/shell printing, as they do not facilitate rapid gelation/cross-linking, which is crucial in this approach.

Disclosures

The authors declare that they have no competing financial interests.

Acknowledgments

The authors would like to acknowledge the financial support for this project received from the Slovenian Research Agency (grant numbers: P3-0036, and I0-0029), and the Ministry of Science, Education and Sport (grant number: 5442-1/2018/59).

References

1. Langer, R., Vacanti, J. Advances in tissue engineering. *Journal of pediatric surgery.* **51** (1), 8-12 (2016).
2. Atala, A., Kasper, F. K., Mikos, A. G. Engineering complex tissues. *Science Translational Medicine.* **4** (160), 160rv112-160rv112 (2012).
3. Khademhosseini, A., Vacanti, J. P., Langer, R. Progress in tissue engineering. *Scientific American.* **300** (5), 64-71 (2009).
4. Wobma, H., Vunjak-Novakovic, G. Tissue Engineering and Regenerative Medicine 2015: A Year in Review. *Tissue Engineering Part B: Reviews.* **22** (2), 101-113 (2016).
5. Park, K. M., Shin, Y. M., Kim, K., Shin, H. Tissue Engineering and Regenerative Medicine 2017: A Year in Review. *Tissue Engineering Part B: Reviews.* **24** (5), 327-344 (2018).
6. Mattei, G., Giusti, S., Ahluwalia, A. Design criteria for generating physiologically relevant in vitro models in bioreactors. *Processes.* **2** (3), 548-569 (2014).
7. Elliott, N. T., Yuan, F. A review of three-dimensional in vitro tissue models for drug discovery and transport studies. *Journal of Pharmaceutical Sciences.* **100** (1), 59-74 (2011).
8. Breslin, S., O'Driscoll, L. Three-dimensional cell culture: the missing link in drug discovery. *Drug Discovery Today.* **18** (5-6), 240-249 (2013).
9. Edmondson, R., Broglie, J. J., Adcock, A. F., Yang, L. Three-dimensional cell culture systems and their applications in drug discovery and cell-based biosensors. *Assay and Drug Development Technologies.* **12** (4), 207-218 (2014).
10. Horvath, P. *et al.* Screening out irrelevant cell-based models of disease. *Nature Reviews Drug Discovery.* **15** (11), 751-769 (2016).
11. Di Nardo, P., Minieri, M., Ahluwalia, A. in *Stem Cell Engineering.* 41-59, Springer (2011).
12. Lee, K., Silva, E. A., Mooney, D. J. Growth factor delivery-based tissue engineering: general approaches and a review of recent developments. *Journal of the Royal Society Interface.* **8** (55), 153-170 (2011).
13. Tayalia, P., Mooney, D. J. Controlled growth factor delivery for tissue engineering. *Advanced Materials.* **21** (32-33), 3269-3285 (2009).
14. Caddeo, S., Boffito, M., Sartori, S. Tissue Engineering Approaches in the Design of Healthy and Pathological In Vitro Tissue Models. *Frontiers in Bioengineering and Biotechnology.* **5,** 40 (2017).
15. Chang, H.-I., Wang, Y. in *Regenerative medicine and tissue engineering-cells and biomaterials.* InTech (2011).
16. Rice, J. J. *et al.* Engineering the regenerative microenvironment with biomaterials. *Advanced Healthcare Materials.* **2** (1), 57-71 (2013).
17. Khademhosseini, A., Langer, R. A decade of progress in tissue engineering. *Nature Protocols.* **11** (10), 1775-1781 (2016).
18. Yu, Y., Alkhawaji, A., Ding, Y., Mei, J. Decellularized scaffolds in regenerative medicine. *Oncotarget.* **7** (36), 58671-58683 (2016).
19. Tibbitt, M. W., Anseth, K. S. Hydrogels as extracellular matrix mimics for 3D cell culture. *Biotechnology and bioengineering.* **103** (4), 655-663 (2009).
20. Lovett, M., Lee, K., Edwards, A., Kaplan, D. L. Vascularization strategies for tissue engineering. *Tissue Engineering Part B: Reviews.* **15** (3), 353-370 (2009).
21. Rouwkema, J., Rivron, N. C., van Blitterswijk, C. A. Vascularization in tissue engineering. *Trends in Biotechnology.* **26** (8), 434-441 (2008).
22. Bae, H. *et al.* Building vascular networks. *Sci Transl Med.* **4** (160), 160ps123, (2012).
23. 23 Štumberger, G., & Vihar, B. Freeform Perfusable Microfluidics Embedded in Hydrogel Matrices. *Materials.* **11** (12), 2529 (2018).
24. Ibrahim, M., Richardson, M. K. Beyond organoids: In vitro vasculogenesis and angiogenesis using cells from mammals and zebrafish. *Reproductive Toxicology.* **73**, 292-311, (2017).
25. Sorrell, J. M., Baber, M. A., Caplan, A. I. Influence of adult mesenchymal stem cells on in vitro vascular formation. *Tissue Engineering Part A.* **15** (7), 1751-1761 (2009).
26. Davies, N. H., Schmidt, C., Bezuidenhout, D., Zilla, P. Sustaining neovascularization of a scaffold through staged release of vascular endothelial growth factor-A and platelet-derived growth factor-BB. *Tissue Engineering Part A.* **18** (1-2), 26-34 (2012).
27. Li, X., He, J., Zhang, W., Jiang, N., Li, D. Additive manufacturing of biomedical constructs with biomimetic structural organizations. *Materials.* **9** (11), 909, (2016).
28. Murphy, S. V., & Atala, A. 3D bioprinting of tissues and organs. *Nature Biotechnology.* **32** (8), 773 (2014).
29. Hasan, A. *et al.* Microfluidic techniques for development of 3D vascularized tissue. *Biomaterials.* **35** (26), 7308-7325 (2014).
30. Kolesky, D. B. *et al.* 3D bioprinting of vascularized, heterogeneous cell-laden tissue constructs. *Advanced Materials.* **26** (19), 3124-3130 (2014).
31. Huang, Y., Zhang, X. F., Gao, G., Yonezawa, T., Cui, X. 3D bioprinting and the current applications in tissue engineering. *Biotechnology Journal.* (2017).
32. Wang, X. *et al.* 3D bioprinting technologies for hard tissue and organ engineering. *Materials.* **9** (10), 802 (2016).
33. Hinton, T. J. *et al.* Three-dimensional printing of complex biological structures by freeform reversible embedding of suspended hydrogels. *Science Advances.* **1** (9), e1500758 (2015).
34. Rocca, M., Fragasso, A., Liu, W., Heinrich, M. A., Zhang, Y. S. Embedded Multimaterial Extrusion Bioprinting. *SLAS Technology.* **23** (2), 154-163 (2018).
35. Hinton, T. J. *et al.* Three-dimensional printing of complex biological structures by freeform reversible embedding of suspended hydrogels. *Science Advances.* **1** (9), e1500758 (2015).
36. Huang, S., Yang, Y., Yang, Q., Zhao, Q., Ye, X. Engineered circulatory scaffolds for building cardiac tissue. *Journal of Thoracic Disease.* **10** (Suppl 20), S2312-s2328 (2018).
37. Hoch, E., Tovar, G. E., & Borchers, K. Bioprinting of artificial blood vessels: current approaches towards a demanding goal. *European Journal of Cardiothoracic Surgery.* **46** (5), 767-778 (2014).
38. Yeo, M., Lee, J. S., Chun, W., Kim, G. H. An Innovative Collagen-Based Cell-Printing Method for Obtaining Human Adipose Stem Cell-Laden Structures Consisting of Core-Sheath Structures for Tissue Engineering. *Biomacromolecules.* **17** (4), 1365-1375 (2016).
39. Liu, W. *et al.* Coaxial extrusion bioprinting of 3D microfibrous constructs with cell-favorable gelatin methacryloyl microenvironments. *Biofabrication.* **10** (2), 024102 (2018).
40. Gao, Q., He, Y., Fu, J. Z., Liu, A., Ma, L. Coaxial nozzle-assisted 3D bioprinting with built-in microchannels for nutrients delivery. *Biomaterials.* **61,** 203-215 (2015).
41. Akkineni, A. R., Ahlfeld, T., Lode, A., Gelinsky, M. A versatile method for combining different biopolymers in a core/shell fashion by 3D plotting to achieve mechanically robust constructs. *Biofabrication.* **8** (4), 045001 (2016).

42. Colosi, C. *et al.* Microfluidic Bioprinting of Heterogeneous 3D Tissue Constructs Using Low-Viscosity Bioink. *Advanced Materials.* **28** (4), 677-684 (2016).
43. Kim, G., Ahn, S., Kim, Y., Cho, Y., Chun, W. Coaxial structured collagen–alginate scaffolds: fabrication, physical properties, and biomedical application for skin tissue regeneration. *Journal of Materials Chemistry.* **21** (17), 6165-6172 (2011).
44. Luo, Y., Lode, A., Gelinsky, M. Direct plotting of three-dimensional hollow fiber scaffolds based on concentrated alginate pastes for tissue engineering. *Advanced Healthcare Materials.* **2** (6), 777-783 (2013).
45. Mistry, P. *et al.* Bioprinting Using Mechanically Robust Core-Shell Cell-Laden Hydrogel Strands. *Macromolecular Bioscience.* **17** (6), (2017).
46. Banović, L., Vihar, B. Development of an extruder for open source 3D bioprinting. *Journal of Open Hardware.* **2** (1), (2018).
47. *HUV-EC-C [HUVEC] (ATCC® CRL-1730™) Homo sapiens umbilical vein.* <http://www.lgcstandards-atcc.org/products/all/CRL-1730.aspx?geo_country=si#documentation> (2019).
48. Habib, A., Sathish, V., Mallik, S., Khoda, B. 3D printability of alginate-carboxymethyl cellulose hydrogel. *Materials.* **11** (3), 454 (2018).
49. Maver, T. *et al.* Combining 3D printing and electrospinning for preparation of pain-relieving wound-dressing materials. *Journal of Sol-Gel Science and Technology.* 1-16 (2018).
50. Kuo, C. K., Ma, P. X. Ionically crosslinked alginate hydrogels as scaffolds for tissue engineering: Part 1. Structure, gelation rate and mechanical properties. *Biomaterials.* **22** (6), 511-521 (2001).
51. Topuz, F., Henke, A., Richtering, W., Groll, J. Magnesium ions and alginate do form hydrogels: a rheological study. *Soft Matter.* **8** (18), 4877-4881 (2012).
52. Perets, A. *et al.* Enhancing the vascularization of three-dimensional porous alginate scaffolds by incorporating controlled release basic fibroblast growth factor microspheres. *Journal of Biomedical Materials Research Part A.* **65** (4), 489-497 (2003).
53. Ruvinov, E., Leor, J., Cohen, S. The effects of controlled HGF delivery from an affinity-binding alginate biomaterial on angiogenesis and blood perfusion in a hindlimb ischemia model. *Biomaterials.* **31** (16), 4573-4582 (2010).
54. Peirce, S. M., Price, R. J., Skalak, T. C. Spatial and temporal control of angiogenesis and arterialization using focal applications of VEGF164 and Ang-1. *American Journal of Physiology-Heart and Circulatory Physiology.* **286** (3), H918-925 (2004).
55. Kageyama, T. *et al.* In situ cross-linkable gelatin-CMC hydrogels designed for rapid engineering of perfusable vasculatures. *ACS Biomaterials Science & Engineering.* **2** (6), 1059-1066 (2016).